A Bioinspired Molybdenum Catalyst for Aqueous Perchlorate Reduction

Changxu Ren, ¹ Peng Yang, ² Jiaonan Sun, ³ Eric Y. Bi, ^{1,4} Jinyu Gao, ¹ Jacob Palmer, ¹ Mengqiang Zhu, ²
Yiying Wu, ³ and Jinyong Liu ^{1,*}

- ¹Department of Chemical and Environmental Engineering, University of California, Riverside, CA 92521, United States.
 - ²Department of Ecosystem Science and Management, University of Wyoming, Laramie, WY 82071, United States.
 - ³Department of Chemistry, The Ohio State University, Columbus, OH 43210, United States.
 - ⁴Martin Luther King High School, Riverside, CA 92508, United States.

9 ABSTRACT

Perchlorate (ClO₄⁻) is a pervasive, harmful, and inert anion on both Earth and Mars. Current technologies for ClO₄⁻ reduction entail either harsh conditions or multi-component enzymatic processes. Herein, we report a heterogeneous (\boldsymbol{L})Mo-Pd/C catalyst directly prepared from Na₂MoO₄, a bidentate nitrogen ligand (\boldsymbol{L}), and Pd/C to reduce aqueous ClO₄⁻ into Cl⁻ with 1 atm H₂ at room temperature. A suite of instrument characterizations and probing reactions suggest that the Mo^{VI} precursor and \boldsymbol{L} at the optimal 1:1 ratio are transformed *in situ* into oligomeric Mo^{IV} active sites at the carbon-water interface. For each Mo site, the initial turnover frequency (TOF₀) for oxygen atom transfer from ClO_x⁻ substrates reached 165 h⁻¹. The turnover number (TON) reached 3,840 after a single batch reduction of 100 mM ClO₄⁻. This study provides a water-compatible, efficient, and robust catalyst to degrade and utilize ClO₄⁻ for water purification and space exploration.

Perchlorate (ClO₄⁻) is a pervasive water contaminant on Earth¹ and a major salt component in the surface soil on Mars.²⁻³ The uptake of ClO₄⁻ through water and food can cause thyroid gland malfunction,⁴ and a recent study has identified that ClO₄⁻ in drinking water is more dangerous than previously thought.⁵ NASA has identified Martian ClO₄⁻ as both a potential hazard to humans and an oxygen source to supply exploration activities.⁶ However, the oxidizing power of ClO₄⁻ is primarily utilized via rocket fuels, munitions, or pyrotechnics.⁷ Without ignition, ClO₄⁻ is a well-known inert anion and commonly used for ionic strength adjustment in various chemical systems.⁸ Abiotic reduction of aqueous ClO₄⁻ usually requires harsh conditions and large excesses of reducing agents.⁹⁻¹⁰ Herein, we report on a bioinspired heterogeneous Mo catalyst for aqueous ClO₄⁻ reduction with 1 atm H₂ at room temperature.

Microbes can use ClO_4^- for respiration via a multifactor metalloenzyme system (Figure 1a). $^{11-12}$ The reduction of ClO_4^- and ClO_3^- is achieved by oxygen atom transfer (OAT) 13 to a dithiolate-coordinated Mo cofactor (Figure 1b), which is biosynthesized from molybdate. 14 Amino acid residues mediate the binding and stabilization of ClO_x^- substrates. 15 The redox cycling between Mo^{IV} and Mo^{VI} (Figure 1c) is sustained by the electron transfer from H_2 or acetate via multiple enzymes containing Fe-S clusters and *heme* complexes, and electron shuttling compounds. 16 The complexity of biological systems challenges the design of an artificial ClO_4^- reduction system, especially in the aqueous phase under ambient conditions. For example, a Fe complex relies on hydrogen bonds in the secondary coordination sphere to reduce ClO_4^- (Figure 1d) and thus requires an anhydrous environment. $^{17-18}$ Moreover, a single-function metal complex or isolated reductase requires special electron donors (e.g., methyl viologen, hydrazine, ferrocene, and phosphine) to sustain the redox cycle of OAT metals. $^{17,19-20}$ Hence, a robust catalyst that can reduce aqueous ClO_4^- with H_2 is highly desirable. $^{21-22}$ Although the immobilization of Re complexes (Figure 1e) $^{23-24}$ onto Pd/C has achieved this function, $^{25-26}$ Re is a rare metal, and the pre-synthesized Re complexes are subject to irreversible decomposition.

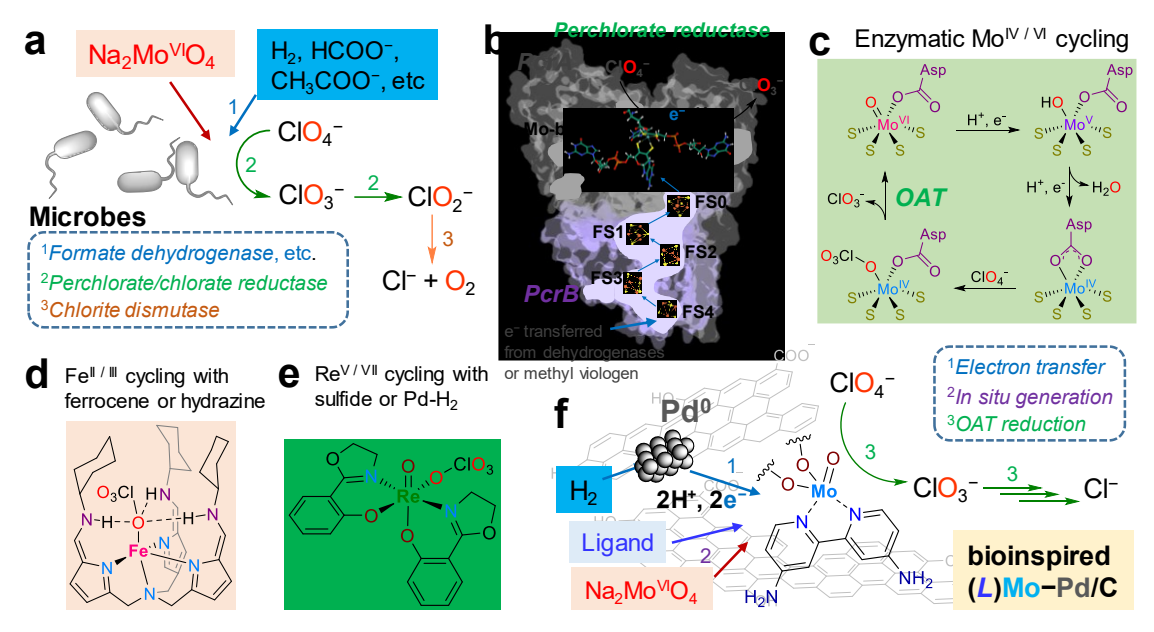


Figure 1. Microbial and abiotic systems for perchlorate reduction. (a) Microbial ClO_4^- reduction processes; (b) electron transfer and metal centers in perchlorate reductase (*Pcr*); (c) redox cycling of the Mo cofactor proposed in literature; ¹⁵ (d) a bioinspired Fe complex for ClO_4^- reduction; ¹⁷ (e) a Re complex for ClO_4^- reduction; ²³ (f) the overall design rationale for the (*L*)MoO_x-Pd/C catalyst.

52

53

54 55

56

57

58

59

60

61

^aReaction conditions: 1 mM ClO₄⁻ in water, 0.5 g L⁻¹ catalyst (5 wt% Mo and 5 wt% Pd on carbon), molar ratio of Ligand:Mo = 1:1 (bidentate and tridentate) or 2:1 (monodentate), pH 3.0, 1 atm H_2 , 20°C. Entries 5 and 6 used 0.2 g L⁻¹ catalyst.

^bCalculated using the degradation of the first 5% of 1 mM ClO₄⁻ and four OAT cycles to reduce each ClO₄⁻ into Cl⁻.

We used Pd/C as the platform for our bioinspired catalyst (Figure 1f). The porous carbon mimics the enzyme protein pocket to accommodate the OAT metal site. The Pd⁰ nanoparticles directly harvest electrons from H₂ to simplify the biological electron transfer chain. Then the critical task was to construct a highly active Mo site from molybdate (Mo^{VI}O₄²⁻), the same Mo source for the biosynthesized Mo cofactor. Polyoxometalates of aqueous molybdate were

readily adsorbed onto Pd/C within 30 min (Figure S1 of the Supporting Information). The resulting heterogeneous MoO_x –Pd/C showed rapid reduction of ClO_3^{-29} but negligible activity with ClO_4^- . Hence, we sought to enhance the OAT activity of Mo sites by incorporating an organic ligand like the biological Mo cofactors. Because biomimetic Mo complexes with thiolate ligands are typically water- and oxygen-sensitive, we attempted to prepare an active Mo site *in situ*. We added Na_2MoO_4 and a variety of neutral nitrogen ligands (L) to the water suspension of Pd/C under 1 atm H_2 . This simple strategy achieved highly active ClO_4^- reduction by a series of (L) MoO_x –Pd/C catalysts (Table 1, Figures S2 and S3).

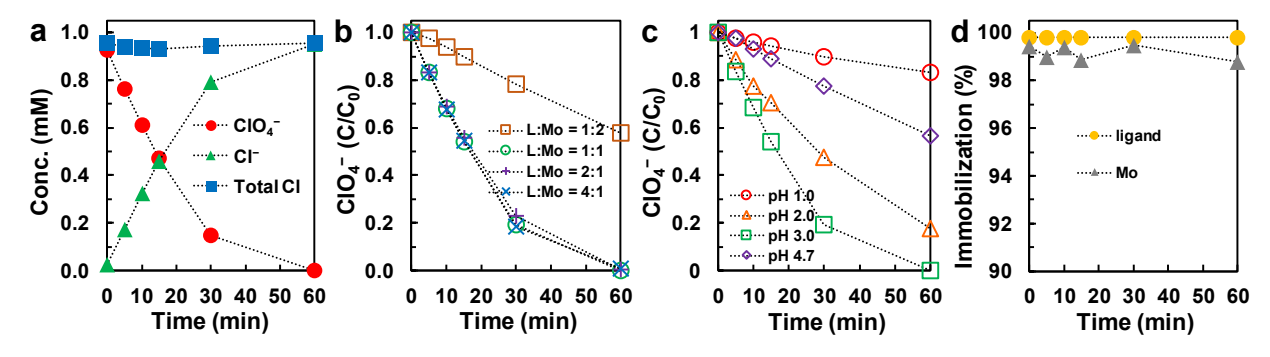


Figure 2. Kinetic data. (a) Chlorine balance for ClO₄⁻ reduction; (b) the effect of (NH₂)₂bpy:Mo molar ratio; (c) the effect of solution pH; (d) the ratio of immobilized (NH₂)₂bpy and Mo during ClO₄⁻ reduction. Default reaction conditions: 0.2 g L⁻¹ catalyst (5 wt% Mo in 5 wt% Pd/C, molar ratio of (NH₂)₂bpy:Mo=1:1), 1 mM ClO₄⁻, pH 3.0, 1 atm H₂, 20 °C.

Bipyridine (bpy, Table 1 entry 1) was superior to phenanthroline and other aromatic ligands with an imidazoline or oxazoline half moiety (Table 1 entries 17-19) as well as pyridines, diamines, and terpyridine (Table 1 entries 10-16 and 23). Ligands with steric hindrance (Table 1 entries 8, 9, and 20) or a strain on the bpy backbone (Table 1 entry 22 versus 21) resulted in low activities. Electron-donating groups on the para positions³⁰ further enhanced the activity (Table 1 entries 2–7). At ambient temperature and pressure, the [(NH₂)₂bpy]MoO_x–Pd/C catalyst (Table 1 entry 6) outperformed other abiotic ClO₄⁻ reduction catalysts reported to date (Table S1). The chlorine balance was closed by ClO₄ and Cl⁻, indicating a negligible buildup of ClO_x intermediates (Figure 2a). The optimal molar ratio between (NH₂)₂bpy and Mo was 1:1 (Figure 2b), and the optimal Mo content in the catalyst was 5 wt% (see below). While enzymes use amino acid residues to assist the reduction of metal-bound oxyanions, 15,31 the [(NH₂)₂bpy]MoO_x-Pd/C needs external protons to enable ClO₄⁻ reduction. ²⁹⁻³⁰ The optimal activity was observed at pH 3.0 (1 mM H⁺ from H₂SO₄). The p K_a values for $-NH_3^+$ and pyridyl NH^+ are around 2 and 7, respectively (Figure S4). The coordination between (NH₂)₂bpv and Mo is competed by the protonation of pyridyl N at pH 3.0. Thus, the active [(NH₂)₂bpy]Mo sites may be in the solid phase rather than in the aqueous solution (see below). The reduced performance at pH 2.0 and 1.0 (Figure 2c) can be attributed to the protonation of -NH₂.

Catalyst reuse for ten times did not cause a noticeable loss of activity (Figure S5). The leached Mo and $(NH_2)_2bpy$ into water throughout the catalysis were <1.5% and <0.2% of the total amount, respectively (Figure 2d). The apparent first-order kinetics with 0.01–1 mM ClO_4^- and zeroth-order kinetics at 1–100 mM ClO_4^- (Figures S6 and S7) support the Langmuir–Hinshelwood model, which is characterisitic for heterogeneous catalysis (See Texts S1 and S2 for kinetic modeling and mass transfer analysis). Notably, a 0.2 g L^{-1} loading of the catalyst reduced 99.99% of 100 mM ClO_4^- (~10 g L^{-1}) within 48 h (Figure S6c). Due to the high oxidative stress caused by

 ClO_x^- intermediates, 15,27 complete reduction of 100 mM ClO_4^- in water has not been reported by either microbial or abiotic systems. Assuming the Mo sites catalyze the OAT from ClO_4^- and all ClO_x^- intermediates, the turnover number (TON) for that single batch and the initial turnover frequency (TOF₀) reached 3,840 and 165 h⁻¹, respectively, for each Mo atom.

In the presence of 0.1 M Cl⁻, 2.0 M Cl⁻, and 1.0 M SO₄²⁻, the catalyst retained 57%, 5%, and 36% of the control activity, respectively (Figure S8 and Table S2), showing the promise for reducing ClO₄⁻ in brine solutions produced from ion exchange or reverse osmosis for water purification.³² Furthermore, exposing the catalyst suspension to air did not cause irreversible deactivation. The same ClO₄⁻ reduction activity was recovered after resuming the H₂ supply (Figure S9a), suggesting that the *in situ* prepared catalyst can be handled in air. In comparison, Re–Pd/C catalysts using pre-synthesized Re^V precursors (Figure 1e) are highly sensitive to air and irreversibly deactivated (Figure S9b).^{25,33}

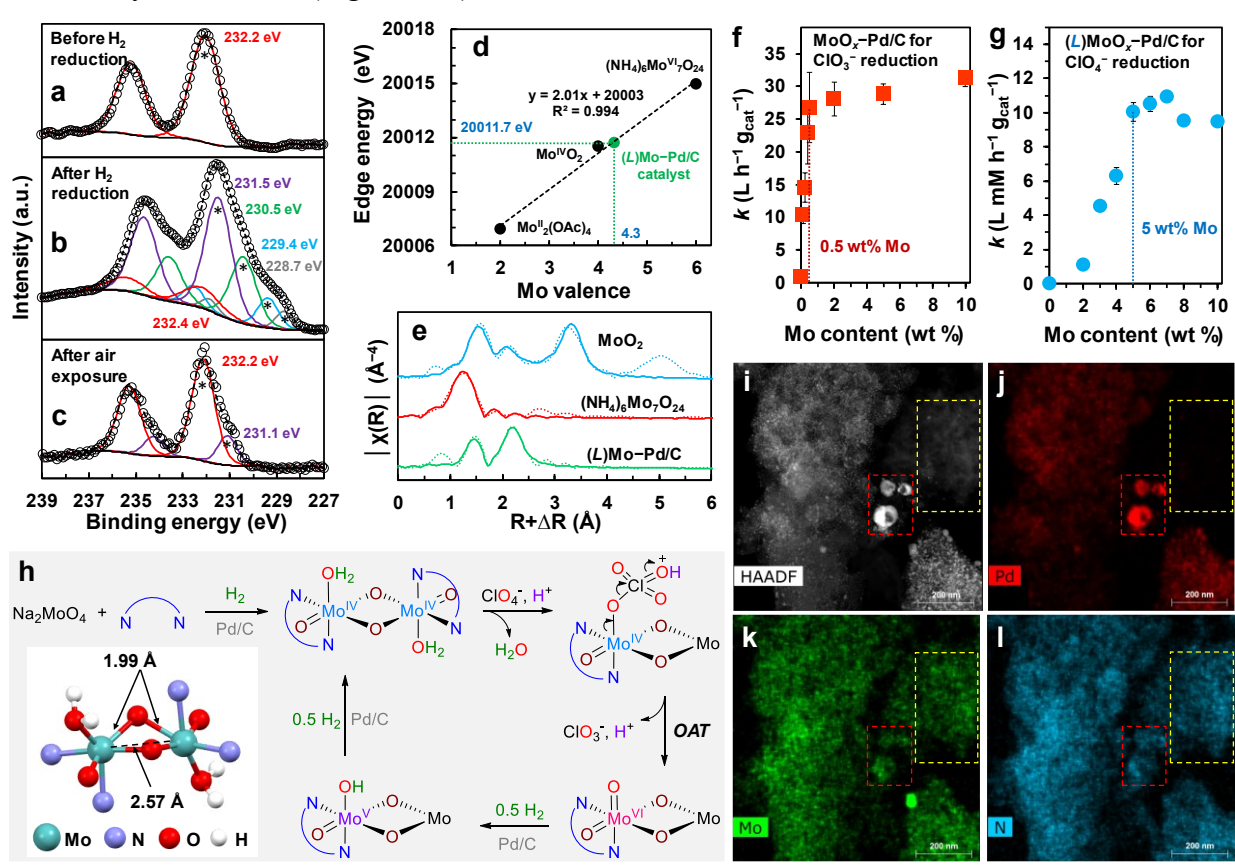


Figure 3. Characterization data and proposed reaction mechanisms. (a–c) Mo 3d XPS spectra (empty dots) and fits (solid lines) of the [(NH₂)₂bpy]MoO_x–Pd/C catalyst. The 3d5/2 peaks are indicated by asterisks; (d) the correlation between Mo K-edge XANES energies and valences for the catalyst and Mo references; (e) the EXAFS Fourier transforms (dotted lines) and their fits (solid lines); (f–g) the effect of Mo content in the catalysts with and without (NH₂)₂bpy; (h) a proposed structure of the reduced [(NH₂)₂bpy]MoO_x species and representative redox transformations for ClO₄⁻ reduction; (i–l) HAADF-STEM imaging of the catalyst and EDX mapping of Pd, Mo, and N. The two dotted areas show the heterogeneity of [(NH₂)₂bpy]MoO_x species immobilized on both the carbon support and Pd particles.

X-ray photoelectron spectroscopy (XPS) characterization identified the reduction of Mo^{VI} precursor into multiple oxidation states (+V, +IV, +III and +II) (Figure 3a versus 3b). Air exposure reoxidized the low-valent species to Mo^V and Mo^{VI} (Figure 3c). For the reduced bulk catalyst sample, Mo K-edge X-ray absorption near-edge structure (XANES) spectroscopic analysis found the average valence of Mo to be 4.3 from the edge energy of 20011.7 eV (Figure 3d and Figure S10)³⁴. Fitting of the extended X-ray absorption fine structure (EXAFS) spectra found three major atomic shells for Mo=O (1.67 Å), Mo=O (1.99 Å) and Mo=Mo (2.57 Å) (Figure 3e, Table S3, and Figure S11). This short Mo=Mo distance also indicates the reduction of Mo^{IV} into Mo^{IV} by hydrogenation. In a previous study, the reduction of [PMo^{VI}₁₂O₄₀]³⁻ in a battery electrolyte with 24 electrons into [PMo^{IV}₁₂O₄₀]²⁷⁻ shortended the Mo=Mo distance from 3.4 Å to 2.6 Å.³⁴ The Mo=Mo coordination number (CN) of 0.9 ± 0.5 suggests the heterogeneity of the surface Mo species as a mixture of monomers (CN = 0), dimers (CN = 1), and polymers (CN > 1).

Notably, the use of $(NH_2)_2bpy$ ligand not only enhanced the activity but also altered the structure of MoO_x species. Without the ligand, the MoO_x –Pd/C catalyst could not reduce ClO_4 –, and the highest ClO_3 – reduction activity was achieved with merely 0.5 wt% of Mo (Figure 3f). Thus, the additional 4.5 wt% of Mo in the 5 wt% MoO_x –Pd/C served as the structural building block of polymeric MoO_x clusters rather than catalytic sites. The CN for Mo–Mo in MoO_x –Pd/C (1.7 \pm 0.6, Table S3) also indicated the dominance of polymeric MoO_x clusters. In stark comparison, the ClO_4 – reduction activity of $[(NH_2)_2bpy]MoO_x$ –Pd/C kept increasing with the Mo content until 5 wt% (Figure 3g). Thus, most Mo atoms in the 5 wt% $[(NH_2)_2bpy]MoO_x$ –Pd/C served as catalytic sites. Because the average CN for Mo–Mo and Mo=O were 0.9 and 1.1, respectively (Table S3) and the optimal ratio between $(NH_2)_2bpy$ and Mo was 1:1 (Figure 2b), we propose a representative dimer structure for the active Mo site (Figure 3h). This configuration is based on the crystal structure of $Mo^{VI}_2O_6[(t-Bu)_2bpy]_2$, a minor product from the hydrothermal reaction using MoO_3 and 4,4– $(t-Bu)_2bpy$. This dimer structure also allows for multi-valent transformation of Mo between +VI and +II (Figure 3b) via the reduction of Mo=O into Mo–OH and Mo–OH₂.

We attempted to synthesize a molecular framework for the [(NH₂)₂bpy]MoO_x site; however, both $[(t-Bu)_2bpv]Mo^{VI}$ and $[(NH_2)_2bpv]Mo^{VI}$ complexes from hydrothermal synthesis³⁵ decomposed into free ligands upon dissolution (Figures S12 and S13). Although PPh3 reduced Mo^{VI} to Mo^{IV} and yielded OPPh₃ by OAT, ¹³ the homogeneous ClO₄⁻ reduction did not occur (Figure S14). The heating of Na₂MoO₄, (NH₂)₂bpy, and P(PhSO₃Na)₃ (TPPTS) in water yielded a green solid, confirming the reduction of Mo^{VI} and the coordination with (NH₂)₂bpy (Figure S15). Still, this product dissolved poorly in water and did not reduce aqueous ClO₄⁻ (Figure S16a). In comparison, the use of activated carbon (without Pd⁰ nanoparticles)³⁶ together with Na₂MoO₄, (NH₂)₂bpv, and TPPTS resulted in a slow but significant ClO₄ reduction at pH 3.0 (Figure S16b and \$16c). Although an exact molecular structure for the active Mo sites remains elusive, the above findings have collectively confirmed the heterogeneous nature of the catalyst. The critical role of the carbon support may be to provide a large surface area (>900 m² g⁻¹)^{29,36} to disperse the insoluble [(NH₂)₂bpy]MoO_x structure for up to 5 wt% Mo (Figure 3g), or to stabilize the specific coordination structure that is reactive with ClO₄⁻. In addition, since (NH₂)₂bpy is strongly prone to pyridyl protonation, the $[(NH_2)_2bpy]MoO_x$ coordination structure is less likely to remain intact upon dissolution in the aqueous phase.

Scanning transmission electron microscopy (STEM) and energy dispersive X-ray spectrometry (EDS) element mapping images indicate the ubiquitous distribution of Mo and N on

either carbon support or Pd⁰ nanoparticles (Figures 3i–3l and S17). The poor EXAFS fittings considering Mo–Pd bonding (Table S4) suggest isolated aggregation and distinct roles of the [(NH₂)₂bpy]MoO_x site (OAT for ClO_x⁻ reduction) and Pd nanoparticles (electron transfer from H₂). Both the phosphine reduction via OAT and Pd-mediated hydrogenation could transform polymeric Mo^{VI} precursors²⁹ into specific [(NH₂)₂bpy]MoO_x structures for ClO₄⁻ reduction. For comparison, our cyclic voltammetry studies on the mixture of Na₂MoO₄, (NH₂)₂bpy, and activated carbon (without Pd⁰ nanoparticles) between 0.37 and –1.1 V (versus the reversible hydrogen electrode) did not observe ClO₄⁻ reduction (Figure S18) but showed the reduction peaks of MoO_x and (NH₂)₂bpy ligand (Figure S19). The potential allows the reduction of Mo^{VI} into Mo^V, Mo^{IV}, and Mo^{III}, ³⁷⁻³⁸ but the potential [(NH₂)₂bpy]MoO_x formed upon electrochemical reduction³⁴ were probably in different structures and thus not reactive with ClO₄⁻.

In conclusion, we have developed a highly active and robust heterogeneous (L)MoO_x–Pd/C catalyst for aqueous ClO₄⁻ reduction. The catalysis proceeded at 20°C with 1 atm H₂ and fully reduced a wide concentration range (10 μ M to 0.1 M) of ClO₄⁻ into Cl⁻. On the carbon support, the oligomeric Mo site was generated *in situ* via the reduction of Na₂MoO₄ and coordination with a bidentate nitrogen ligand. This study highlights a new strategy for designing bioinspired systems with common chemicals and simple preparation. We anticipate that this water-compatible catalyst will advance environmental and energy technologies to degrade or utilize ClO₄⁻ on Earth and Mars.

ASSOCIATED CONTENT

Supporting Information

- The Supporting Information is available free of charge at
- https://pubs.acs.org/doi/10.1021/jacs.xxxxxxx.
- Methods for catalyst preparation, perchlorate reduction, aqueous sample analysis, catalyst
- characterization, electrochemical study; supporting texts for Langmuir-Hinshelwood mechanism,
- mass transfer analysis, and mechanism probing studies using phosphine; supporting data figures
- for metal and ligand leaching, the effect of ligand structures, catalyst reuse and air stability, kinetics
- under various conditions, characterization data of XANES, EXAFS, HAADF-STEM-EDX; photos
- and NMR spectra for mechanism probing studies; cyclic voltammograms; supporting data tables
- for comparison with other catalysts, kinetics, and EXAFS fittings.

AUTHOR INFORMATION

Corresponding Author

- *(J.L.) E-mail: jinyongl@ucr.edu; jinyong.liu101@gmail.com.
- 199 **Notes**

166

167

168169

170

171

172

173

174

175

176

177

178

179

180

181

182

183 184

185

186

187

196

197

198

201

The authors declare no competing financial interest.

ACKNOWLEDGMENTS

- Dr. Krassimir Bozhilov assisted STEM characterization at the Central Facility for Advanced
- 203 Microscopy and Microanalysis (CFAMM) at UC Riverside. Dr. Ich Tran assisted XPS
- 204 characterization at the UC Irvine Materials Research Institute (IMRI). Funding: UC Riverside

- startup grant and the National Science Foundation (NSF) Division of Chemical, Bioengineering, 205
- Environmental, and Transport Systems, Environmental Engineering Program (CBET-1932942) 206
- for C.R., E.B., J.P., and J.L.; the U.S. Department of Energy (DOE) Experimental Program to 207
- Stimulate Competitive Research (DOE-EPSCoR DE-SC0016272) for P.Y. and M.Z.; NSF 208
- Division of Chemistry, Chemical Catalysis Program (CHE-1566106) for J.S. and Y.W. The use of 209
- Stanford Synchrotron Radiation Lightsource at SLAC National Accelerator Laboratory was 210
- supported by the U.S. DOE, Office of Science, Office of Basic Energy Sciences (DE-AC02-211
- 76SF00515). The XPS facility at IMRI was funded in part by NSF Major Research Instrumentation 212
- Program (CHE-1338173). 213

REFERENCES

- 215 Brandhuber, P.; Clark, S.; Morley, K. A review of perchlorate occurrence in public drinking water systems. J. Am. Water Works Assoc. 2009, 101, 63-73. 216
 - Hecht, M.; Kounaves, S.; Quinn, R.; West, S.; Young, S.; Ming, D.; Catling, D.; Clark, B.; Boynton,
- W. V.; Hoffman, J. Detection of perchlorate and the soluble chemistry of martian soil at the Phoenix lander 218
- 219 site. Science 2009, 325, 64-67.
- 220 Jackson, W. A.; Davila, A. F.; Sears, D. W.; Coates, J. D.; McKay, C. P.; Brundrett, M.; Estrada,
- 221 N.; Böhlke, J. K. Widespread occurrence of (per)chlorate in the Solar System. Earth Planet. Sci. Lett. 2015,
- *430*, 470-476. 222

214

217

- Greer, M. A.; Goodman, G.; Pleus, R. C.; Greer, S. E. Health effects assessment for environmental 223
- perchlorate contamination: The dose response for inhibition of thyroidal radioiodine uptake in 224
- humans. Environ. Health Perspect. 2002, 110, 927-937. 225
- Llorente-Esteban, A.; Manville, R. W.; Reyna-Neyra, A.; Abbott, G. W.; Amzel, L. M.; Carrasco, 226
- N. Allosteric regulation of mammalian Na⁺/I⁻ symporter activity by perchlorate. Nat. Struct. Mol. Biol. 227
- **2020**, 27, 533-539. 228
- 6. Davila, A. F.; Willson, D.; Coates, J. D.; McKay, C. P. Perchlorate on Mars: A chemical hazard 229
- and a resource for humans. Int. J. Astrobiol. 2013, 12, 321-325. 230
- Rehwoldt, M. C.; Yang, Y.; Wang, H.; Holdren, S.; Zachariah, M. R. Ignition of nanoscale 231
- titanium/potassium perchlorate pyrotechnic powder: Reaction mechanism study. J. Phys. Chem. C 2018, 232
- *122*, 10792-10800. 233
- Gayen, P.; Sankarasubramanian, S.; Ramani, V. K. Fuel and oxygen harvesting from Martian 234
- regolithic brine. Proc. Natl. Acad. Sci. U. S. A. 2020, 117, 31685-31689. 235
- Gu, B.; Dong, W.; Brown, G. M.; Cole, D. R. Complete degradation of perchlorate in ferric chloride 236
- and hydrochloric acid under controlled temperature and pressure. Environ. Sci. Technol. 2003, 37, 2291-237
- 238 2295.
- 239 10. Cao, J.; Elliott, D.; Zhang, W.-x. Perchlorate reduction by nanoscale iron particles. J. Nanopart.
- Res. 2005, 7, 499-506. 240
- Coates, J. D.; Achenbach, L. A. Microbial perchlorate reduction: Rocket-fuelled metabolism. Nat. 241
- Rev. Microbiol. 2004, 2, 569-580. 242
- Youngblut, M. D.; Wang, O.; Barnum, T. P.; Coates, J. D. (Per)chlorate in biology on earth and 243
- beyond. Annu. Rev. Microbiol. 2016, 70, 435-457. 244
- Holm, R. Metal-centered oxygen atom transfer reactions. Chem. Rev. 1987, 87, 1401-1449. 245 13.
- 246 14. Schwarz, G.; Mendel, R. R.; Ribbe, M. W. Molybdenum cofactors, enzymes and pathways. *Nature*
- **2009**, 460, 839. 247

- 248 15. Youngblut, M. D.; Tsai, C.-L.; Clark, I. C.; Carlson, H. K.; Maglaqui, A. P.; Gau-Pan, P. S.;
- Redford, S. A.; Wong, A.; Tainer, J. A.; Coates, J. D. Perchlorate reductase is distinguished by active site
- aromatic gate residues. J. Biol. Chem. **2016**, 291, 9190-9202.
- 251 16. Bertero, M. G.; Rothery, R. A.; Palak, M.; Hou, C.; Lim, D.; Blasco, F.; Weiner, J. H.; Strynadka,
- N. C. Insights into the respiratory electron transfer pathway from the structure of nitrate reductase A. *Nat.*
- 253 Struct. Mol. Biol. **2003**, 10, 681-687.
- 254 17. Ford, C. L.; Park, Y. J.; Matson, E. M.; Gordon, Z.; Fout, A. R. A bioinspired iron catalyst for
- nitrate and perchlorate reduction. *Science* **2016**, *354*, 741-743.
- 256 18. Drummond, M. J.; Miller, T. J.; Ford, C. L.; Fout, A. R. Catalytic perchlorate reduction using iron:
- Mechanistic insights and improved catalyst turnover. ACS Catal. 2020, 10, 3175-3182.
- Hutchison, J. M.; Poust, S. K.; Kumar, M.; Cropek, D. M.; MacAllister, I. E.; Arnett, C. M.; Zilles,
- J. L. Perchlorate reduction using free and encapsulated Azospira oryzae enzymes. *Environ. Sci. Technol.*
- **2013**, *47*, 9934-9941.
- 261 20. Elrod, L. T.; Kim, E. Lewis acid assisted nitrate reduction with biomimetic molybdenum
- 262 oxotransferase complex. *Inorg. Chem.* **2018**, *57*, 2594-2602.
- 263 21. Yin, Y. B.; Guo, S.; Heck, K. N.; Clark, C. A.; Coonrod, C. L.; Wong, M. S. Treating water by
- degrading oxyanions using metallic nanostructures. ACS Sustain. Chem. Eng. 2018, 6, 11160-11175.
- 265 22. Chaplin, B. P.; Reinhard, M.; Schneider, W. F.; Schüth, C.; Shapley, J. R.; Strathmann, T. J.; Werth,
- C. J. Critical review of Pd-based catalytic treatment of priority contaminants in water. *Environ. Sci. Technol.* 267
 2012, 46, 3655-3670.
- 23. Abu-Omar, M. M.; McPherson, L. D.; Arias, J.; Béreau, V. M. Clean and efficient catalytic reduction of perchlorate. *Angew. Chem.* **2000**, *112*, 4480-4483.
- 270 24. Liu, J.; Wu, D.; Su, X.; Han, M.; Kimura, S. Y.; Gray, D. L.; Shapley, J. R.; Abu-Omar, M. M.;
- Werth, C. J.; Strathmann, T. J. Configuration control in the synthesis of homo- and heteroleptic bis
- 272 (oxazolinylphenolato/thiazolinylphenolato) chelate ligand complexes of oxorhenium(V): Isomer effect on
- ancillary ligand exchange dynamics and implications for perchlorate reduction catalysis. *Inorg. Chem.* **2016**,
- *55*, 2597-2611.
- 25. Liu, J.; Choe, J. K.; Wang, Y.; Shapley, J. R.; Werth, C. J.; Strathmann, T. J. Bioinspired complex-
- 276 nanoparticle hybrid catalyst system for aqueous perchlorate reduction: Rhenium speciation and its influence
- on catalyst activity. *ACS Catal.* **2015**, *5*, 511-522.
- 278 26. Liu, J.; Han, M.; Wu, D.; Chen, X.; Choe, J. K.; Werth, C. J.; Strathmann, T. J. A new bioinspired
- 279 perchlorate reduction catalyst with significantly enhanced stability via rational tuning of rhenium
- coordination chemistry and heterogeneous reaction pathway. *Environ. Sci. Technol.* **2016**, *50*, 5874-5881.
- 281 27. Liu, J.; Chen, X.; Wang, Y.; Strathmann, T. J.; Werth, C. J. Mechanism and mitigation of the
- decomposition of an oxorhenium complex-based heterogeneous catalyst for perchlorate reduction in water.
- 283 Environ. Sci. Technol. **2015**, 49, 12932-12940.
- 28. Oyerinde, O. F.; Weeks, C. L.; Anbar, A. D.; Spiro, T. G. Solution structure of molybdic acid from
- Raman spectroscopy and DFT analysis. *Inorg. Chim. Acta* **2008**, *361*, 1000-1007.
- 286 29. Ren, C.; Yang, P.; Gao, J.; Huo, X.; Min, X.; Bi, E. Y.; Liu, Y.; Wang, Y.; Zhu, M.; Liu, J. Catalytic
- reduction of aqueous chlorate with MoO_x Immobilized on Pd/C. ACS Catal. 2020, 10, 8201-8211.
- 30. Hurley, K. D.; Zhang, Y.; Shapley, J. R. Ligand-enhanced reduction of perchlorate in water with
- 289 heterogeneous Re–Pd/C catalysts. *J. Am. Chem. Soc.* **2009**, *131*, 14172-14173.
- 290 31. Mirts, E. N.; Petrik, I. D.; Hosseinzadeh, P.; Nilges, M. J.; Lu, Y. A designed heme-[4Fe-4S]
- metalloenzyme catalyzes sulfite reduction like the native enzyme. *Science* **2018**, *361*, 1098-1101.
- 292 32. Liu, J.; Choe, J. K.; Sasnow, Z.; Werth, C. J.; Strathmann, T. J. Application of a Re–Pd bimetallic
- catalyst for treatment of perchlorate in waste ion-exchange regenerant brine. *Water Res.* **2013**, *47*, 91-101.

- 294 33. Zhang, Y.; Hurley, K. D.; Shapley, J. R. Heterogeneous catalytic reduction of perchlorate in water 295 with Re–Pd/C catalysts derived from an oxorhenium(V) molecular precursor. *Inorg. Chem.* **2011**, *50*, 1534-296 1543.
- 297 34. Wang, H.; Hamanaka, S.; Nishimoto, Y.; Irle, S.; Yokoyama, T.; Yoshikawa, H.; Awaga, K. In operando X-ray absorption fine structure studies of polyoxometalate molecular cluster batteries: Polyoxometalates as electron sponges. *J. Am. Chem. Soc.* **2012**, *134*, 4918-4924.
- 35. Amarante, T. R.; Neves, P.; Paz, F. A. A.; Pillinger, M.; Valente, A. A.; Gonçalves, I. S. A dinuclear oxomolybdenum(VI) complex, [Mo₂O₆(4,4'-di-tert-butyl-2,2'-bipyridine)₂], displaying the {MoO₂(μ-O)₂MoO₂}⁰ core, and its use as a catalyst in olefin epoxidation. *Inorg. Chem. Commun.* **2012**, *20*, 147-152.
- 36. Gao, J.; Ren, C.; Huo, X.; Ji, R.; Wen, X.; Guo, J.; Liu, J. Supported palladium catalysts: A facile preparation method and implications to reductive catalysis technology for water treatment. *ACS ES&T Eng.* **2021**, *1*, 562–570.
- 37. Anbananthan, N.; Rao, K. N.; Venkatesan, V. Cyclic voltammetric investigations of the reduction of Mo(VI) to Mo(IV) in 1 M sulphuric acid. *J. Electroanal. Chem.* **1994**, *374*, 207-214.
- 308 38. You, J.; Wu, D.; Liu, H. Electrochemical studies of molybdate and thiomolybdates. *Polyhedron* 1986, 5, 535-537.

310 **TOC Graphic**

311

